J|A|C|S
ARTICLES
Published on Web 04/14/2007

Photochromism of Diarylethene Single Molecules in Polymer Matrices

Tuyoshi Fukaminato,† Tohru Umemoto,† Yasuhide Iwata,† Satoshi Yokojima,‡ Mitsuru Yoneyama,‡ Shinichiro Nakamura,‡ and Masahiro Irie*,†

Contribution from the Department of Chemistry and Biochemistry, Graduate School of Engineering, Kyushu University, Hakozaki 6-10-1, Higashi-ku, Fukuoka 812-8581, Japan, and Mitsubishi Chemical Group, Science and Technology Research Center, Inc. and CREST-JST, 1000 Kamoshida-cho, Aoba-ku, Yokohama 227-8502, Japan

Received December 20, 2006; E-mail: iriem@rikkyo.ac.jp

Abstract: Robust fluorescent photoswitching molecules, having perylene bisimide as the fluorescent unit and diarylethene as the switching unit, were prepared, and their photochromic reactions were measured at the single-molecule level in various polymer matrices. The histograms of the fluorescent on and off times were found to deviate from normal exponential distribution and showed a peak when the molecules are embedded in rigid polymer matrices, such as Zeonex or poly(methyl methacrylate) (PMMA). In soft polymer matrices, such as poly(*n*-buthyl methacrylate) (PnBMA), exponential distribution was observed for the on and off times. The abnormal distribution suggests that the quantum yields of the photoreactions are not constant and the molecules undergo the reactions after absorbing a certain number of photons. A multilocal minima model was proposed to explain the environmental effect.

Introduction

Recent advances in fluorescence microscopy have allowed detection, imaging, and spectroscopy of single molecules at room temperature.[1−19] The single molecule detection technique is useful not only to probe microenvironments[15,20−26] but also to characterize the photochemical reactivity of individual molecules.[27] The detailed analysis of the reactivity of each molecule is indispensable to develop ultrahigh-density single-

† Kyushu University.

‡ Mitsubishi Chemical Group, Science and Technology Research Center, Inc. and CREST-JST.

(1) Examples of reviews and special issues for single molecule detection: (a) Ambrose, W. P.; Goodwin, P. M.; Jett, J. H.; Orden, A. V.; Werner, J. H.; Keller, R. A. *Chem. Rev.* **1999**, *99*, 2929−2956. (b) Xie, X. S.; Trautman, J. K. *Annu. Rev. Phys. Chem.* **1998**, *49*, 441−480. (c) Tamarat, P.; Maali, A.; Lounis, B.; Orrit, M. *J. Phys. Chem. A* **2000**, *104*, 1−16. (d) Moerner, W. E. *J. Phys. Chem. B* **2002**, *106*, 910−927. (e) Basché, T.; Moerner, W. E.; Orrit, M.; Wild, U. P. *Single-Molecule Optical Detection, Imaging and Spectroscopy*; Wiely-VCH: Weinheim, Germany, 1997. (f) Rigler, R.; Orrit, M.; Basché, T. *Single Molecule Spectroscopy-Nobel Conference Lecture*; Springer-Verlag: Berlin, Heidelberg, Germany, 2001. (g) Kraayenhof, R.; Visser, A. J. W. G.; Gerritsen, H. C. *Fluorescence Spectroscopy, Imaging and Probes-New Tools in Chemical, Physical and Life Sciences*; Springer-Verlag: Berlin, Heidelberg, Germany, 2002. (h) Zander, C.; Enderlein, J.; Keller, R. A. *Single Molecule Detection in Solution: Method and Application*; Wiely-VCH: Weinheim, Germany, 2002. (i) Tinnefeld, P.; Sauer, M. *Angew. Chem., Int. Ed.* **2005**, *44*, 2642−2671.
(2) Betzig, E.; Chichester, R. J. *Science* **1993**, *262*, 1422−1425.
(3) Nie, S.; Chiu, D. T.; Zare, R. N. *Science* **1994**, *266*, 1018−1021.
(4) Trautman, J. K.; Macklin, J. J.; Brus, L. E.; Betzig, E. *Nature* **1994**, *369*, 40−42.
(5) Ambrose, W. P.; Goodwin, P. M.; Martin, J. C.; Keller, R. A. *Science* **1994**, *265*, 364−367.
(6) Moerner, W. E. *Science* **1994**, *265*, 46−53.
(7) Xie, X. S.; Dunn, R. C. *Science* **1994**, *265*, 361−364.
(8) Basché, T.; Kummer, S.; Bräuchle, C. *Nature* **1995**, *373*, 132−134.
(9) Macklin, J. J.; Trautman, J. K.; Harris, T. D.; Brus, L. E. *Science* **1996**, *272*, 255−258.
(10) Lu, H. P.; Xie, X. S. *Nature* **1997**, *385*, 143−146.
(11) Ha, T.; Enderle, T.; Chemla, D. S.; Selvin, P. R.; Weiss, S. *Phys. Rev. Lett.* **1996**, *77*, 3979−3982.
(12) Lu, H. P.; Xun, L.; Xie, X. S. *Science* **1998**, *282*, 1877−1882.
(13) Veerman, J. A.; Garcia-Parajo, M. F.; Kuipers, L.; van Hulst, N. F. *Phys. Rev. Lett.* **1999**, *83*, 2155−2158.
(14) (a) Vanden Bout, D. A.; Yip, W. T.; Hu, D. H.; Fu, D. K.; Swager, T. M.; Barbara, P. F. *Science* **1997**, *277*, 1074−1077. (b) Yu, J.; Hu, D.; Barbara, P. F. *Science* **2000**, *289*, 1327−1330.
(15) Deschenes, L. A.; Vanden Bout, D. A. *Science* **2001**, *292*, 255−258.
(16) Hofkens, J.; Maus, M.; Gensch, T.; Vosch, T.; Cotlet, M.; Köhn, F.; Herrmann, A.; Müllen, K.; De Schryver, F. C. *J. Am. Chem. Soc.* **2000**, *122*, 9278−9288.
(17) Dickson, R. M.; Cubitt, A. B.; Tsien, R. Y.; Moerner, W. E. *Nature* **1997**, *388*, 355−358.
(18) Kulzer, F.; Kummer, S.; Matzke, R.; Bräuchle, C.; Basché, T. *Nature* **1997**, *387*, 688−691.
(19) Funatsu, T.; Harada, Y.; Tokunaga, M.; Saito, K.; Yanagida, T. *Nature* **1995**, *374*, 555−559.
(20) (a) Deschenes, L. A.; Vanden Bout, D. A. *J. Phys. Chem. B* **2002**, *106*, 11438−11445. (b) Deschenes, L. A.; Vanden Bout, D. A. *J. Phys. Chem. B* **2001**, *105*, 11978−11985.
(21) (a) Wang, H.; Bardo, A. M.; Collinson, M. M.; Higgins, D. A. *J. Phys. Chem. B* **1998**, *102*, 7231−7237. (b) Mei, E.; Bardo, A. M.; Collinson, M. M.; Higgins, D. A. *J. Phys. Chem. B* **2000**, *104*, 9973−9980. (c) Seebacher, C.; Hellriegel, C.; Bräuchle, C.; Ganschow, M.; Wöhrle, D. *J. Phys. Chem. B* **2003**, *107*, 5445−5452. (d) Hellriegel, C.; Kirstein, J.; Bräuchle, C.; Latour, V.; Pigot, T.; Olivier, R.; Lacombe, S.; Brown, R.; Guieu, V.; Payrastre, C.; Izquierdo, A.; Mocho, P. *J. Phys. Chem. B* **2004**, *108*, 14699−14709. (e) Hellriegel, C.; Kirstein, J.; Bräuchle, C. *New J. Phys.* **2005**, *7*, 23.
(22) Weston, K. D.; Carson, P. J.; Metiu, H.; Buratto, S. K. *J. Chem. Phys.* **1998**, *109*, 7474−7485.
(23) Osborne, M. A.; Barnes, C. L.; Balasubramanian, S.; Klenerman, D. *J. Phys. Chem. B* **2001**, *105*, 3120−3126.
(24) Vallée, R. A. L.; Tomczak, N.; Kuipers, L.; Vancso, G. J.; van Hulst, N. F. *Phys. Rev. Lett.* **2003**, *91*, 038301−1-038304.
(25) (a) Schmidt, Th.; Schütz, G. J.; Baumgartner, W.; Gruber, H. J.; Schindler, H. *J. Phys. Chem.* **1995**, *99*, 17662−17668. (b) Talley, C. E.; Dunn, R. C. *J. Phys. Chem. B* **1999**, *103*, 10214−10220.
(26) Vallée, R. A. L.; Cotlet, M.; Van der Auweraer, M.; Hofkens, J.; Müllen, K.; De Schryver, F. C. *J. Am. Chem. Soc.* **2004**, *126*, 2296−2297.
(27) (a) Heilemann, M.; Margeat, E.; Kasper, R.; Sauer, M.; Tinnefeld, P. *J. Am. Chem. Soc.* **2005**, *127*, 3801−3806. (b) Mei, E.; Vinogradov, S.; Hochstrasser, R. M. *J. Am. Chem. Soc.* **2003**, *125*, 13198−13204. (c) Habuchi, S.; Ando, R.; Dedecker, P.; Verheijen, W.; Mizuno, H.; Miyawaki, A.; Hofkens, J. *Proc. Natl. Acad. Sci. U.S.A.* **2005**, *102*, 9511−9516. (d) Roeffaers, M. B. J.; Sels, B. F.; Uji-i, H.; De Schryver, F. C.; Jacobs, P. A.; De Vos, D. E.; Hofkens, J. *Nature* **2006**, *439*, 572−575.

10.1021/ja069131b CCC: $37.00

Scheme 1. Fluorescent Photochromic Molecule **1** and **2**

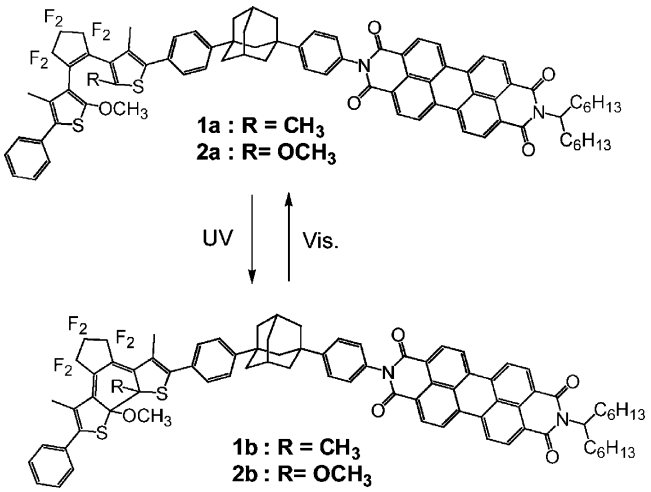

molecule optical memory[17,18,28,29] (each molecule stores 1 bit of optical information) as well as photoswitching devices. Although we recently reported on the on/off digital fluorescence switching of single photochromic molecules embedded in a polymer film by irradiation with UV and visible light,[29] the analysis of the reaction mechanism was incomplete because of lack of photostability of the chromophores used. The number of switching cycles was limited to a few cycles. The histograms of the photochemical events shown in the papers[29] were constructed by collecting many molecules in different microenvironments. It is required to synthesize highly stable photochromic molecules, which enable us to follow the photochromism of the same molecule many times (>100 times) in the same microenvironment.

Recently, we have succeeded to synthesize robust fluorescent photochromic diarylethene derivatives **1** and **2** (Scheme 1), which undergo efficient and stable photochromic reactions.[30] The molecules have large absorption coefficients, high fluorescence quantum yields, and photostability. The excellent characteristic properties opened detailed discussions of photochromic reactions at the single-molecule level. In this study, we measured the photochromic reactions in various polymer matrices and analyzed the reactivity at the single-molecule level. We found a novel environmental effect in the photochromic reactions of the single molecules.

Results and Discussion

Molecular Design of Fluorescent Photochromic Molecules. In a previous paper,[29] we prepared fluorescent photochromic diarylethenes having a bis(phenylethynyl)anthracene unit. Although the molecules were successfully used to demonstrate photoswitching of fluorescence at the single-molecule level, the fluorescent anthracene unit decomposed after a few cycles before the decomposition of the diarylthene switching unit. For the detailed analysis of the photochromic reactions at the single-molecule level, it is required to develop a robust fluorescent photochromic molecule, which enables us to follow the photochromic reactions many times without decomposition. As candidates of such molecules, we designed and synthesized fluorescent diarylethene derivatives having perylene bisimide as shown in Scheme 1.

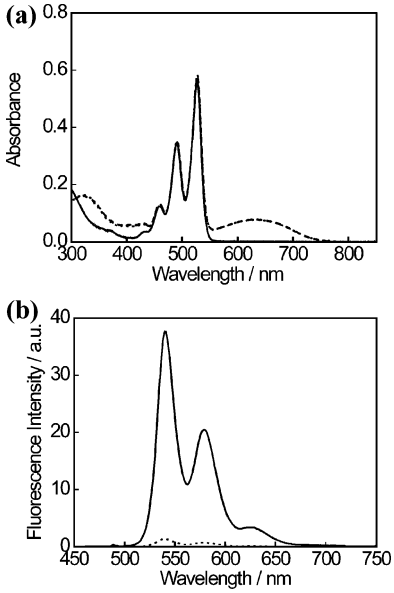

Figure 1. (a) Absorption and (b) fluorescence spectra in dichloromethane solution of **2** ($C = 6.6 \times 10^{-6}$ M) upon 313 nm light irradiation: (—) open-ring isomer, (· · · · ·) photostationary state, (− − − −) closed-ring isomer.

The perylene bisimide unit was chosen as the fluorescent unit because of its high fluorescence quantum yield (~1.0), large molecular extinction coefficient (88 000 M^{-1} cm^{-1} at λ_{max}), and photostability.[31] The diarylethenes contain one (**1a**) or two (**2a**) methoxy groups at the reactive carbons. The methoxy group controls the cycloreversion quantum yield.[32]

Figure 1 shows absorption and fluorescence spectral changes of **2** upon irradiation with UV light in dichloromethane. Fluorescence intensity of both compounds (**1** and **2**) decreases when the diarylethene unit converts from the open- to the closed-ring isomers.[30] In order to know the fluorescence quenching mechanism,[33] the fluorescence quantum yield of **1** was measured in hexane, toluene, and ethyl acetate solutions. The fluorescence quantum yields were determined to be 0.98, 0.96, and 0.97, respectively, by utilizing *N*,*N*′-bis(1-hexylheptyl)perylene-3,4,9,-10-tetracarboxyl bisimide in toluene as a reference ($\Phi_f \approx 1.0$). The constant fluorescence quantum yield irrespective of solvent polarity indicates that the contribution of electron transfer is negligible in the quenching process.

The reversible fluorescence intensity change is ascribed to the intramolecular energy transfer switching as shown in Figure 2. When the diarylethene unit is in the open-ring form, the perylene bisimide unit gives strong fluorescence because the energy state of the diarylethene unit is higher than the fluorescent state. When the diarylethene unit converts to the closed-ring

(28) (a) Irie, M. *Photo-Reactive Materials for Ultrahigh-Density Optical Memory*; Elsevier: Amsterdam, The Netherlands, 1994. (b) Irie, M. *Chem. Rev.* **2000**, *100*, 1685.
(29) (a) Irie, M.; Fukaminato, T.; Sasaki, T.; Tamai, N.; Kawai, T. *Nature* **2002**, *420*, 759−760. (b) Fukaminato, T.; Sasaki, T.; Kawai, T.; Tamai, N.; Irie, M. *J. Am. Chem. Soc.* **2004**, *126*, 14843−14849.
(30) Fukaminato, T.; Umemoto, T.; Iwata, Y.; Irie, M. *Chem. Lett.* **2005**, *34*, 676−677.
(31) Langhals, H. *Helv. Chem. Acta* **2005**, *88*, 1309−1343.
(32) (a) Shibata, K.; Kobatake, S.; Irie, M. *Chem. Lett.* **2001**, *30*, 618−619. (b) Morimitsu, K.; Shibata, K.; Kobatake, S.; Irie, M. *J. Org. Chem.* **2002**, *67*, 4574−4578.
(33) (a) Lor, M.; Thielemans, J.; Viaene, L.; Cotlet, M.; Hofkens, J.; Weil, T.; Hampel, C.; Müllen, K.; Verhoeven, J. W.; Van der Auweraer, M.; De Schryver, F. C. *J. Am. Chem. Soc.* **2002**, *124*, 9918−9925. (b) Holman, M. W.; Liu, R.; Adams, D. M. *J. Am. Chem. Soc.* **2003**, *125*, 12649−12654.

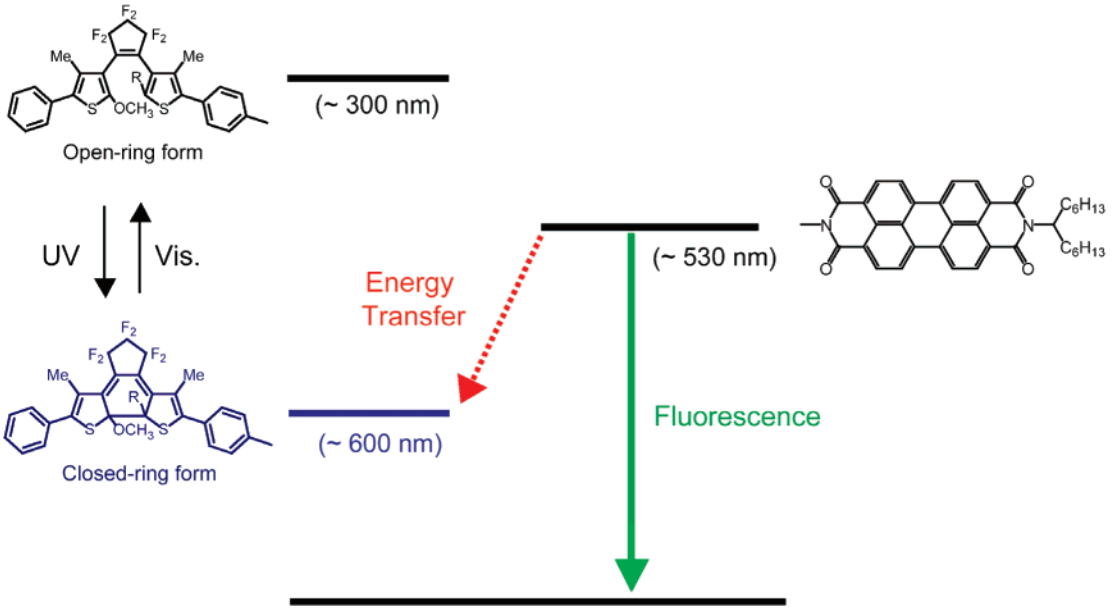

Figure 2. Fluorescence energy transfer switching based on photochromic reaction of diarylethene derivatives.

Table 1. Photocyclization ($\Phi_{o\rightarrow c}$), Photocycloreversion ($\Phi_{c\rightarrow o}$) Quantum Yields of **1** and **2**, and Fluorescence Properties of Compounds **1**, **2**, and *N*,*N*′-Bis(1-hexylheptyl)perylene-3,4,9,10-tetracarboxyl Bisimide in Dichloromethane

compound	$\Phi_{o\rightarrow c}$[a]	$\Phi_{c\rightarrow o}$	$\lambda_{f,max}$/nm	Φ_f	τ/ns
1a	0.26	–	489, 525	0.98	4.1
1b	–	1.4×10^{-3} [b]	–	<0.001	$(4.5 \pm 1.5) \times 10^{-3}$
2a	0.13	–	489, 526	0.97	3.9
2b	–	4.1×10^{-5} [c]	–	<0.001	*d*
N,*N*′-bis(1-hexylheptyl)-perylene-3,4,9,10-tetracarboxyl bisimide	–	–	490, 526	1.0	4.0

[a] Measured by irradiation with 343 nm light. [b]Measured with 592 nm light. [c]Measured with 622 nm light. [d]Not determined.

form, the state becomes lower than the fluorescent state and the fluorescence of the perylene bisimide unit is efficiently quenched. The fluorescence lifetime measurement confirmed this mechanism. The fluorescence lifetime of the open-ring form was measured to be 4.1 ns. The lifetime decreased to less than 5 ps when the diarylethene unit converts to the closed-ring form, as shown in Table 1. Very efficient intramolecular energy transfer took place in the molecule. Similar fluorescence switching was also observed for compound **2**.

The cyclization/cycloreversion quantum yields of **1** and **2** were also measured and summarized in Table 1. The cyclization quantum yield was determined by comparing the photocyclization rates of samples and furyl-fulgide with the standard procedure.[34] **1a** and **2a** have similar cyclization quantum yields, but the cycloreversion quantum yields are markedly different. The cycloreversion quantum yield of **2b** is 1% of that of **1b**. The decrease in the quantum yield is attributed to the methoxy substituent effect at the reactive carbons.[32]

Photochromism at the Single-Molecule Level. Typical fluorescence intensity trajectories for **2a** and **1a** are shown in Figure 3a and 3b, respectively. The sample for the single-molecule measurement was prepared by spin-coating a toluene solution of the dye (compound **1** or **2**; around 10^{-11} M) and polymer (Zeonex, PMMA, PnBMA, and Arton; around 2 wt %) on a quartz cover glass at 4000 rpm. The closed-ring isomers of the diarylethene derivatives (**1b** and **2b**) were isolated by HPLC and used as the dye. When the closed-ring isomers are

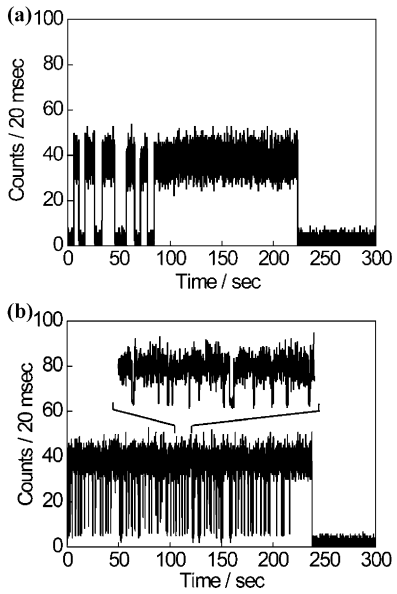

Figure 3. Fluorescence intensity trajectories of (a) **2** and (b) **1** embedded on Zeonex thin films (~100 nm) irradiated with both 488 nm light (fixed power, 100 W/cm^2) and weak 325 nm light (270 μW/cm^2) simultaneously. The long lasting on-state from 90 s is ascribed to the fluorescence of perylene bisimide alone after the decomposition of the diarylethene unit.

(34) (a) Yokoyama, Y.; Kurita, Y. *J. Synth. Org. Chem. Jpn.* **1991**, *49*, 364−372. (b) Hellar, H. G.; Langan, J. R. *J. Chem. Soc., Perkin Trans. 2* **1981**, 341−343.

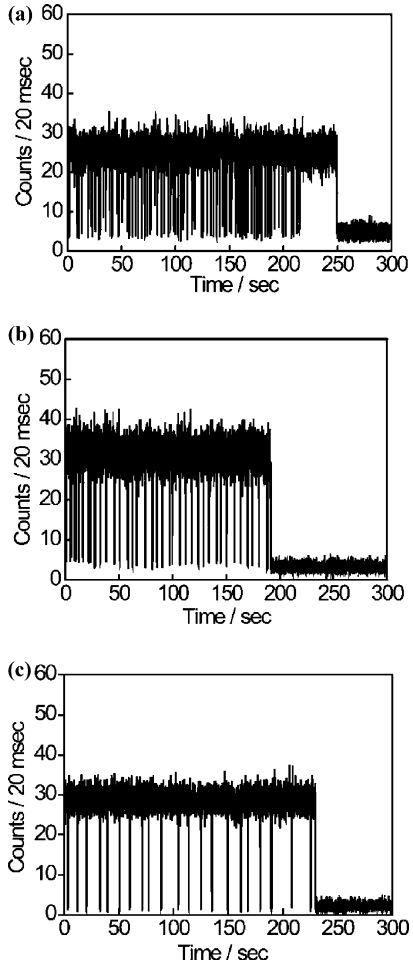

Figure 4. Time traces of fluorescence intensity of **1** embedded in a Zeonex thin film irradiated with both 488 nm light (fixed power, 100 W/cm^2) and 325 nm light (variable power): (a) 270 μW/cm^2, (b) 54 μW/cm^2, (c) 27 μW/cm^2.

dispersed in the polymer matrices, the conformation of the molecules is fixed in photoactive antiparallel one, even after conversion to the open-ring isomers. The antiparallel conformation is a necessary condition for the molecules to undergo the photocyclization reaction.[35] Both compounds showed one-step photobleaching as is expected for a single molecule. The average detected photon numbers of fluorescence before decomposition were around 5×10^5, which indicates excellent photostability of these molecules.

The fluorescence switching was performed under irradiation with both 488 nm (100 W/cm^2) and 325 nm (270 μW/cm^2) light. Although the switching could be repeated more than a few cycles for compound **2a**, the cycle was limited to less than 10 times because the cycloreversion quantum yield of **2b** is very small ($\Phi_{c\rightarrow o} = 4.1 \times 10^{-5}$). On the other hand, the cycles around 100 times were observed for compound **1a**.[30] The switching is not a physical blinking phenomenon. The frequency was reduced upon decreasing the UV power from 270 μW/cm^2 to 27 μW/cm^2 as shown in Figure 4, which indicates that the switching is due to the reversible photochromic reactions. The switching cycles dramatically increased in comparison with previous molecules. Based on the analysis of 100 molecules, the average possible switching cycles of **1** in the same microenvironment were estimated to be around 100.

In the above experiment amorphous polyolefine (Zeonex, $T_g \approx 130$ °C) was used as the host polymer matrix. To know the effect of environment on the photochromic reaction, two more polymers, which have different T_g values, were examined. One is poly(methyl methacrylate) (PMMA) having a T_g of 105 °C, and the other is poly(*n*-buthylmethacrylate) (PnBMA) having a T_g of 21 °C. To reveal the detailed photochemical reactivity of individual molecules in these polymer matrices, the time traces of single molecule **1b** were measured under irradiation with both visible (488 nm, 100 W/cm^2) and weak UV (325 nm, 270 μW/cm^2) light.

The fluorescence intensity switching between two discrete states was observed in all polymer matrices. Figure 5 shows an example of the on and off histograms observed for a single molecule in Zeonex. The on and off states are clearly discriminated as shown in Figure 5b. Figure 5c and 5d show the histograms of on and off times, respectively. The on as well as off histogram showed a peak at a certain on or off time. Although exponential distribution is anticipated from the simple photochemical events, this was not the case. The abnormal distribution of the histograms was observed in most of the molecules (>80%), and the shapes were very similar among the molecules. Any remarkable difference in the distribution between the early events (0−100 s) and later events (100−200 s) was not observed.

The shapes of the histograms are dependent on the polymer matrices as shown in Figure 6. In Zeonex and PMMA matrices, the histograms show a peak at a certain on or off time. On the other hand, in PnBMA, the on- and off-time histograms are normal exponential shapes as shown in Figure 6b and 6e. In PnBMA, with T_g being below or nearly equal to the measuring temperature, the embedded molecules are considered not to be strictly fixed and freely rotate in the polymer matrix. The result suggests that the abnormal histogram is ascribed to the rigidity of the polymer matrices. When the polymer matrices have high T_g values and are rigid enough, the molecules showed the abnormal histograms. This was further confirmed by using a polymer (modified Arton-amorphous polyolefin) having extremely high T_g values ($T_g = 300$ °C) as shown in Figure 6c and 6f. The difference in the histograms will be discussed in the following section.

Environmental Effect of the Reactions. The appearance of the peak in the histogram suggests that the quantum yield of the molecule is not constant and increases with an increasing number of absorbed photons. In other words, the molecule remembers the number of absorbed photons and undergoes the reaction after absorbing a certain number of photons. A possible explanation for the abnormal histograms is given by the multilocal minima model, as shown in Figure 7. The polymer chains surrounding the diarylethene molecule work as the steric hindrance. The effect of the steric hindrance will be reflected on the potential energy surface as (i) deepening the potential minima and creating the higher barriers and (ii) creating additional local minima. These local minima may exist not only for the ground state but also for the excited states. If the created potential barriers are large enough, the thermally induced motion to other local minima will be prevented and the optical excitation

(35) (a) Uchida, K.; Nakayama, Y.; Irie, M. *Bull. Chem. Soc. Jpn.* **1990**, *63*, 1311−1315. (b) Irie, M.; Miyatake, O.; Uchida, K. *J. Am. Chem. Soc.* **1992**, *114*, 8715−8716.

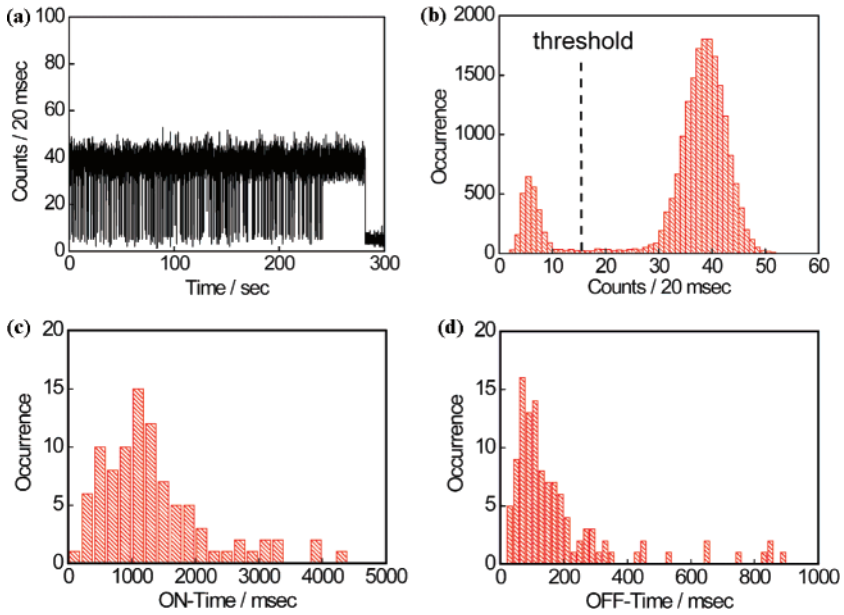

Figure 5. Analysis of single-molecule photochromism in a Zeonex thin film irradiated with both 488 nm light (fixed power, 100 W/cm^2) and 325 nm light (270 μW/cm^2): (a) Time trace of fluorescence intensity of **1**. (b) Histogram of fluorescence photoncounts during bin time (20 ms). The dashed line represented the threshold value between on and off levels. (c) Histogram of on time. (d) Histogram of off time.

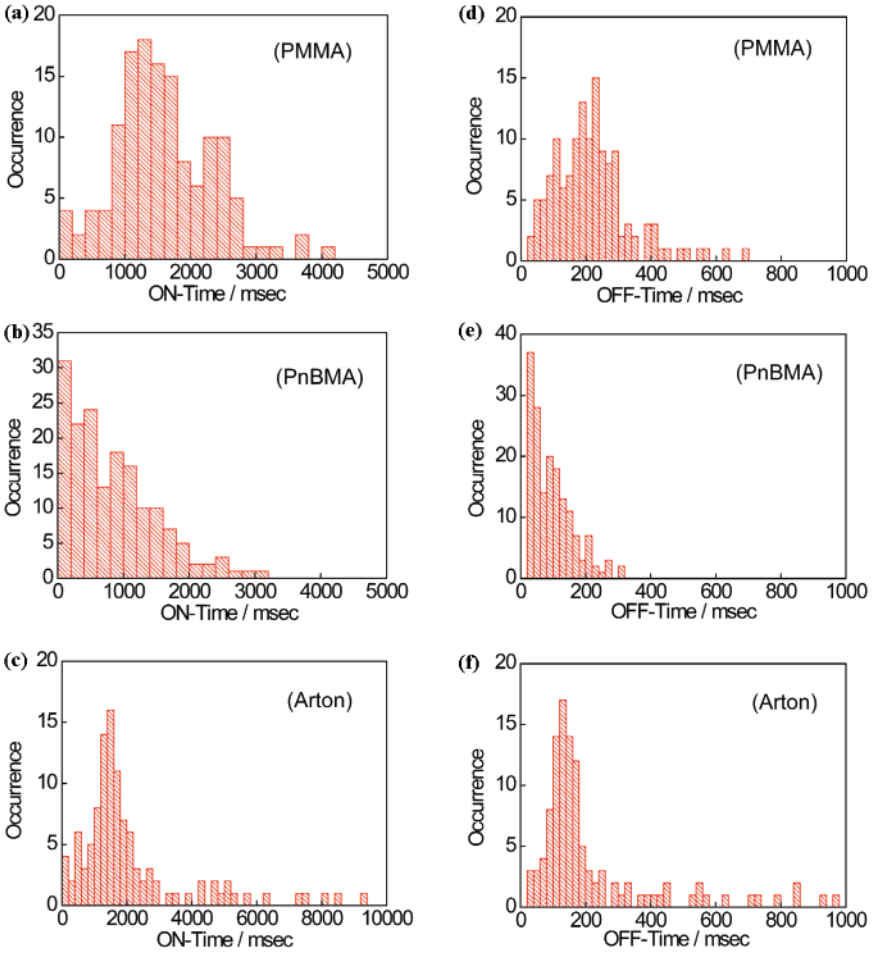

Figure 6. Histograms of (a−c) on time and (d−f) off time in PMMA (a, d), PnBMA (b, e), and Arton (c, f). The histograms were constructed from the time trace of fluorescence intensity of **1** in polymer matrices irradiated with both 488 nm light (fixed power, 100 W/cm^2) and 325 nm light (270 μW/cm^2).

is required to go to other local minima. After the photoexcitation, the open- or closed-ring isomer tries to switch to the closed- or open-ring isomer, but the motion is prevented by a local minimum in the excited state. Then, it may experience the nonradiative decay and will be trapped by the local minimum nearby. Thus, it requires many steps for the molecule to undergo the reaction from open- (or closed-) to closed- (or open-) isomers.

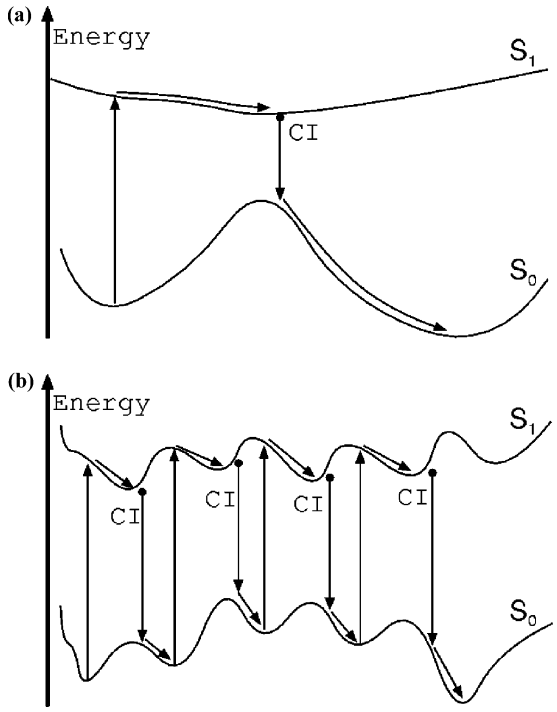

Figure 7. A schematic diagram of the potential energy surface of diarylethene (a) in the gas phase and (b) in the polymer matrix.

It is possible to reproduce the environmental effect from this model as follows. We assume that there are n local minima and the probability to go to the next local minimum after the excitation is p_f. The probability to stay on the same local minimum after the excitation is $1 - p_f$. Then, the probability $P_n(N)$ to induce the reaction for the first time after the N-th excitation can be written as

$$P_n(N) = \begin{cases} {}_{N-1}C_{n-2}\, p_f^{n-1}(1-p_f)^{N-n+1} & (N \geq n-1) \\ 0 & (N < n-1) \end{cases} \quad (1)$$

The corresponding quantum yield $Y_n(N)$ for the N-th excitation can be written as

$$Y_n(N) = \frac{P_n(N)}{1 - \sum_{i=1}^{N-1} P_n(i)}$$

$$= \begin{cases} \dfrac{{}_{N-1}C_{n-2}\, p_f^{n-1}}{\sum_{i=0}^{n-2} {}_{N-1}C_i\, p_f^i (1-p_f)^{n-2-i}} & (N \geq n-1) \\ 0 & (N < n-1) \end{cases} \quad (2)$$

From eq 2, it is easy to show that $\lim_{N\to\infty} Y_n(N) = p_f$. For $p_f = 0.5$, we plot $Y_n(N)$ and $P_n(N)$ (Figure 8). Here, we further assume that the number of excitation N is the normalized number of absorbed photons, which is approximately corresponding to the on or off time. In Figure 8, $n = 2$ corresponds to the system where there is no other local minima except the open- and closed-ring isomers. Thus, the quantum yield in Figure 8a shows the constant value p_f for $n = 2$. This is reflected in Figure 8b as

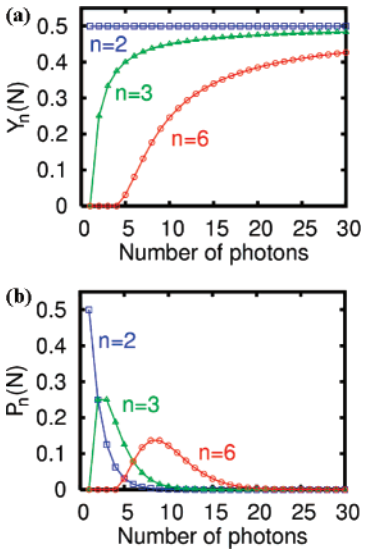

Figure 8. Number of excitation dependence of the cyclization/cycloreversion reactions. (a) The yield $Y_n(N)$ to induce the reaction for the N-th excitation in the n-local minima system. (b) The probability $P_n(N)$ to induce the reaction for the first time after the N-th excitation in the n-local minima system. The blue line with squares was for the two local minima, which are open- and closed-ring isomers. The green line with triangles was for the three local minima. The red line with circles was for the six local minima.

the exponential decay of $P_n(N)$. This is normal behavior observed in PnBMA. The yield for the N-th excitation is no longer a constant for $n > 2$ (see Figure 8a). It starts from zero and monotonically increases to approach p_f as the number of excitations increases. The larger the number of local minima n, the slower the yield to approach p_f. Figure 8b, which corresponds to the experimental histograms for the on/off time, shows a peak for $n = 3$. The profiles for $n = 3-6$ resemble the experimental profiles of the on or off times. Another but similar explanation is given by a model with a time-dependent potential energy surface. For example, if the potential barrier in the excited-state decreases whenever the diarylethene absorbs the photon, we can obtain similar graphs as shown in Figure 8.

Conclusions.

Single-molecule photochromic reactions in various polymer matrices were measured and analyzed by utilizing robust fluorescent diarylethene derivatives. We found a novel environmental effect in the photochromic reactions of the single-molecules. In order to explain the effect, we proposed a multi-local minima model. The multi-local minima model successfully reproduced the novel effect.

Experimental Section

Materials. Detailed synthetic procedures of compound **1a** and **2a** were described in the Supporting Information. The molecules were purified by GPC and HPLC carefully. The molecular structure was confirmed by ^{1}H NMR, elemental analysis, and mass spectroscopy, and purity was evaluated by HPLC. The closed-ring isomers **1b** and **2b** were prepared by irradiating the cyclohexane or toluene solutions with UV light and purified by HPLC.

Single-Molecule Detection. Samples for single-molecule measurements were prepared by spin-coating 2×10^{-11} M toluene solution of the closed-ring isomers (**1b** and **2b**) isolated

by HPLC on a quartz cover glass coating with each polymer film (50−100 nm) at 4000 rpm.

A single-molecule experiment was carried out at ambient temperature using a confocal microscope (TCS−NT, Leica), equipped with a 100×, 1.4 NA objective lens (Leica PL APO CS, NA 1.4). The sample was excited with circularly polarized 488 nm light from an argon ion laser (Spectra Physics Stabilite 2017), and the fluorescence was collected and guided through the appropriate notch (Kaiser Optical) and long-pass (Chroma) filters. A pinhole was placed in the detection path to decrease the focal depth. The fluorescence passed through a long-pass filter (>500 nm) was detected by using single-photon-counting avalanche photodiode (APD) detector (Perkin-Elmer/EG & G, AQR-14). The fluorescence intensity transients were measured with a bin time of 20 ms. Very weak UV light (325 nm, 270 μW/cm^2) from a He−Cd laser (KINMON ELECTRIC, IK3151R-E) was used for the photocyclization reaction. All measurements were performed under a nitrogen atmosphere.

Acknowledgment. This work was partly supported by a Grant-In-Aid for Fundamental Research Program (S) (No. 15105006), Grant-in-Aid for Young Scientist (B) (No. 18750119), Grant-in-Aid for Scientific Research on Priority Areas (432) (No. 16072214) from the Ministry of Education, Culture, Sports, Science, and Technology (MEXT) of Japanese Government, and also by CREST, JST.

Note Added after ASAP Publication. After this paper was published ASAP April 14, 2007, a typographical error was corrected in the lower index of the summation in the second part of eq 2. The corrected version was published ASAP April 19, 2007.

Supporting Information Available: Detailed synthetic procedures for all compounds and the derivation of the equation for multilocal minima model. This material is available free of charge via the Internet at http://pubs.acs.org.

JA069131B